Electronic Supplementary Information

Radical chain mechanism for the $S_2O_8^{2-}$ – $S_2O_3^{2-}$ – Cu(II) flow system explains high-amplitude pH oscillations in the NH₄OH-modified version

Krisztina Kurin-Csörgei, István Szalai and Miklós Orbán

Laboratory of Nonlinear Chemical Dynamics, Institute of Chemistry, Eötvös University,

Pázmány Péter sétány 1/A, Budapest 1117, Hungary

Derivation of the kinetic differential equations

Rate laws:

$v_1=k_1[S_2O_3^{2-}][Cu^{2+}]$

$v_2=k_2[S_2O_3^{-}]^2$

$v_3=k_3[S_2O_8^{2-}][Cu^{+}]$

$v_4=k_4[SO_4^{-}]^2$

$v_5=k_5[SO_4^{-}]$

$v_6=k_6[S_2O_3^{2-}][OH\cdot]$

$v_7=k_7[S_2O_8^{2-}][SO_4^{-}]$

$v_8=k_8[S_2O_8^{-}]$

$v_9=k_9[S_2O_3^{-}][O_2][H^{+}]$

$v_{10}=k_{10}[OH\cdot]^2$

$v_{11}=k_{11}[S_2O_8^{2-}][H_2O_2]$

$v_{12}=k_{12}[S_2O_3^{-}][SO_4^{-}]$

$v_{13}=k_{13}[S_2O_3^{2-}][S_2O_3SO_4^{2-}]$

$v_{14}=k^f_{14}[HSO_4^{-}]- k^b_{14}[H^{+}][SO_4^{2-}]$

$v_{15}=k^f_{15}[H^{+}][OH^{-}]- k^b_{15}$

$v_{16}=k^f_{16}[NH_3]- k^b_{16}[NH_4^{+}][OH^{-}]$

Differential equations for the simulations of the CSTR behavior:

$d[S_2O_3^{2-}]/dt=-v_1-v_6-v_{13}+k_0([S_2O_3^{2-}]_0-[S_2O_3^{2-}])$

$d[Cu^{2+}]/dt=-v_1+v_3+k_0([Cu^{2+}]_0-[Cu^{2+}])$

$d[S_2O_3^{-}]/dt=v_1-2v_2+v_6-v_9-v_{12}+k_0([S_2O_3^{-}]_0-[S_2O_3^{-}])$

$d[Cu^{+}]/dt=v_1-v_3+k_0([Cu^{+}]_0-[Cu^{+}])$

$d[S_4O_6^{2-}]/dt=v_2+v_{13}+k_0([S_4O_6^{2-}]_0-[S_4O_6^{2-}])$

$d[S_2O_8^{2-}]/dt=-v_3+v_4-v_7-v_{10}+k_0([S_2O_8^{2-}]_0-[S_2O_8^{2-}])$

$d[SO_4^{-}]/dt=v_3-2v_4-v_5-v_7+2v_8-v_{12}+k_0([SO_4^{-}]_0-[SO_4^{-}])$

$d[SO_4^{2-}]/dt=v_3+v_{14}+v_7+v_{13}+k_0([SO_4^{2-}]_0-[SO_4^{2-}])$

$d[HSO_4^{-}]/dt=-v_{14}+v_5+2v_{11}+k_0([HSO_4^{-}]_0-[HSO_4^{-}])$

$d[OH\cdot]/dt= v_5-v_6+v_8-2v_{10}+k_0([OH\cdot]_0-[OH\cdot])$

$d[H^{+}]/dt=--v_{15}+v_{14}-v_9+v_8+k_0([H^{+}]_0-[H^{+}])$

$d[OH^{-}]/dt=-v_{15}+v_6+v_{16}+k_0([OH^{-}]_0-[OH^{-}])$

$d[S_2O_8^{-}]/dt=v_7-v_8+k_0([S_2O_8^{-}]_0-[S_2O_8^{-}])$

$d[O_2]/dt=-v_9+v_{11}+k_0([O_2]_0-[O_2])$

$d[H_2O_2]/dt=v_{10}-v_{11}+k_0([H_2O_2]_0-[H_2O_2])$

$d[S_2O_3SO_4^{2-}]/dt=v_{12}-v_{13}+k_0([S_2O_3SO_4^{2-}]_0-[S_2O_3SO_4^{2-}])$

$d[HN_3]/dt=-v_{16}+k_0([HN_3]_0-[HN_3])$

$d[HN_4^{+}]/dt=v_{16}+k_0([HN_4^{+}]_0-[HN_4^{+}])$

Supplementary Figures
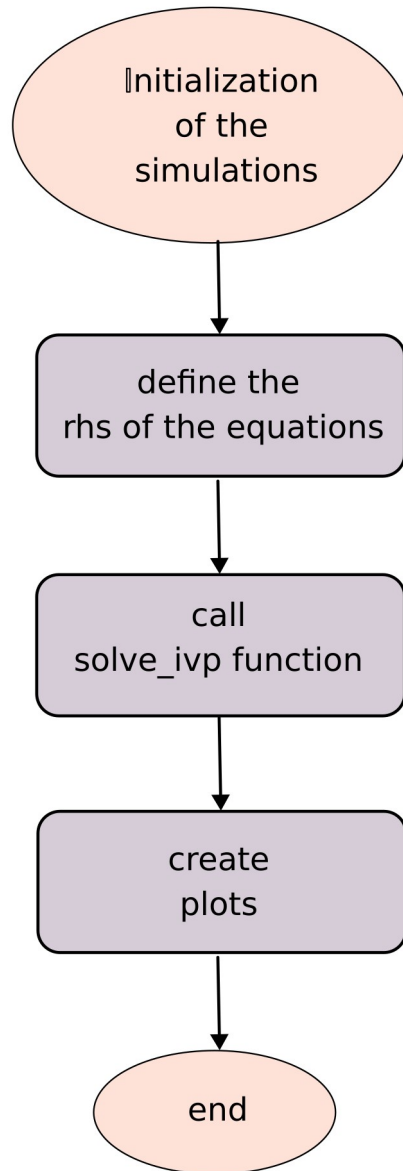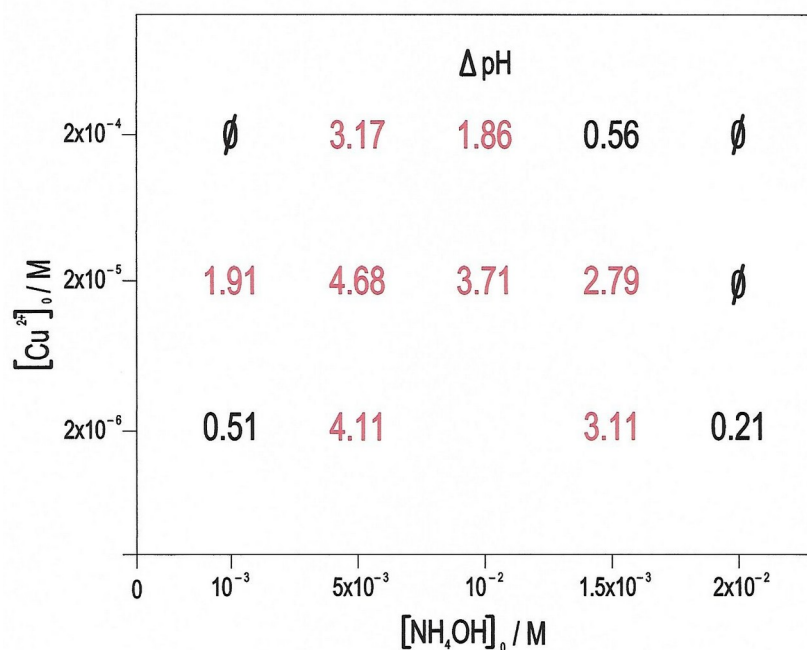

Figure S1. Flowhart of the numerical simulations.

Figure S2. Amplitude of the high amplitude pH oscillations (ΔpH) in the $[Cu^{2+}]_0 - [NH_4OH]_0$ plane at fixed $[S_2O_8^{2-}] = 0.02$ M, $[S_2O_3^{2-}] = 0.005$ M, $k_0 = 2 \times 10^{-3}$, T = 25 °C.

ΔpH data, $[Cu^{2+}]_0$ / M (vertical) vs $[NH_4OH]_0$ / M (horizontal):

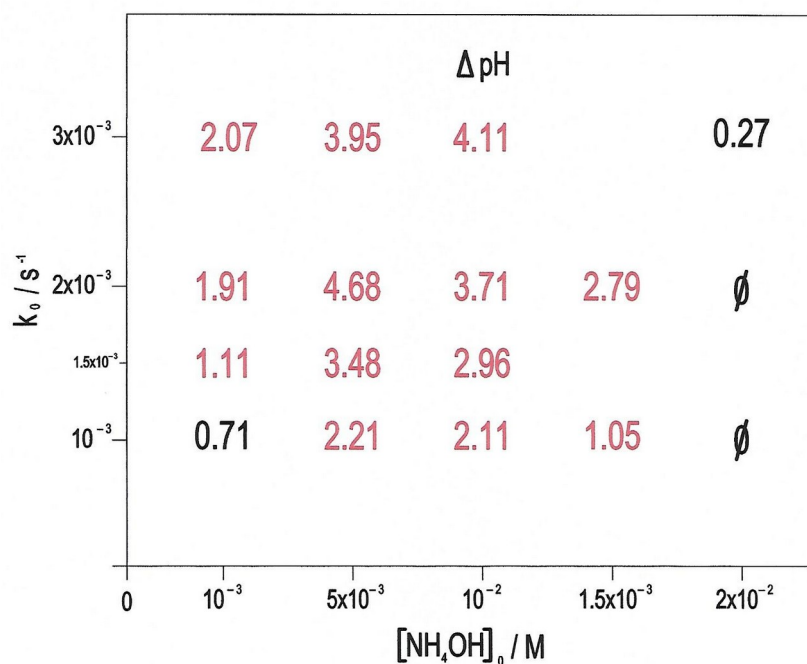| $[Cu^{2+}]_0$ / M	10^{-3}	5×10^{-3}	10^{-2}	1.5×10^{-2}	2×10^{-2}
2×10^{-4}	∅	3.17	1.86	0.56	∅
2×10^{-5}	1.91	4.68	3.71	2.79	∅
2×10^{-6}	0.51	4.11		3.11	0.21

Figure S3. Amplitude of the high amplitude pH oscillations (ΔpH) in the $(k_0) - [NH_4OH]_0$ plane at fixed $[S_2O_8^{2-}] = 0.02$ M, $[S_2O_3^{2-}] = 0.005$ M, $[Cu^{2+}] = 2 \times 10^{-5}$ M, T = 25 °C.

ΔpH data, k_0 / s^{-1} (vertical) vs $[NH_4OH]_0$ / M (horizontal):

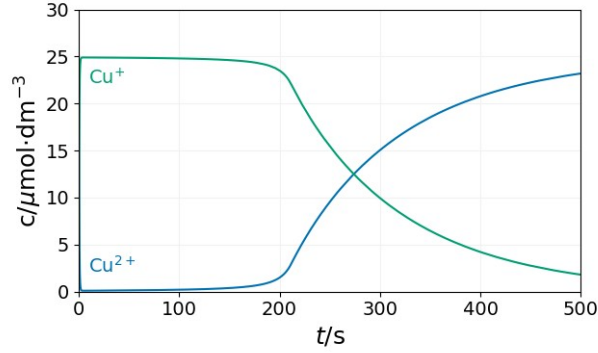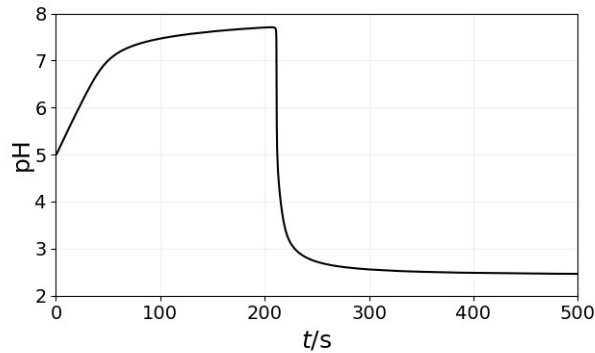| k_0 / s^{-1}	10^{-3}	5×10^{-3}	10^{-2}	1.5×10^{-2}	2×10^{-2}
3×10^{-3}	2.07	3.95	4.11		0.27
2×10^{-3}	1.91	4.68	3.71	2.79	∅
1.5×10^{-3}	1.11	3.48	2.96		
10^{-3}	0.71	2.21	2.11	1.05	∅

Figure S4. Simulation of the batch dynamics of the peroxodisulfate-thiosulfate-copper(II) reaction. The parameters used in the simulations are: $[S_2O_3^{2-}]_0 = 0.0025$ M, $[S_2O_8^{2-}]_0 = 0.025$ M, $[Cu^{2+}]_0 = 2.5 \times 10^{-5}$ M, $[H^+]_0 = 10^{-5}$ M.
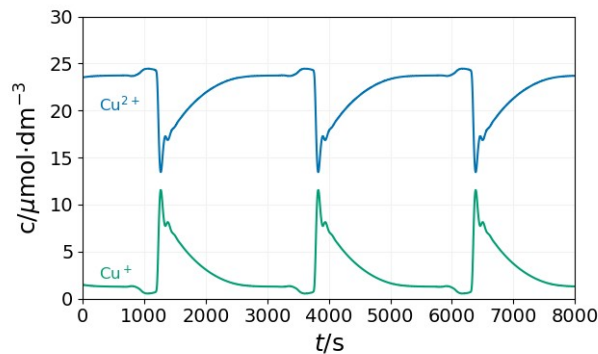

Figure S5. Simulation of the batch dynamics of the peroxodisulfate-thiosulfate-copper(II) reaction. The parameters used in the simulations are: $[S_2O_3^{2-}]_0 = 0.0025$ M, $[S_2O_8^{2-}]_0 = 0.025$ M, $[Cu^{2+}]_0 = 2.5 \times 10^{-5}$ M, $[H^+]_0 = 10^{-5}$ M.
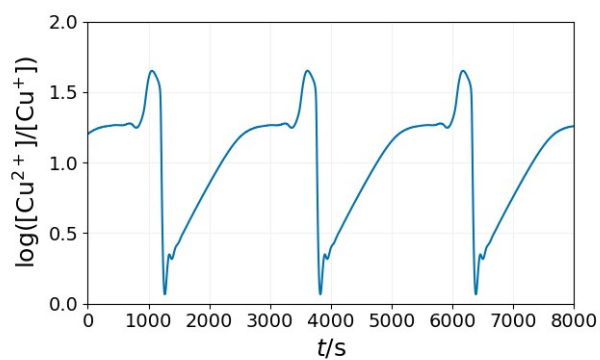

Figure S6. Simulation of the CSTR dynamics of the peroxodisulfate-thiosulfate-copper(II) reaction. The parameters used in the simulations are: $[S_2O_3^{2-}]_0 = 0.0025$ M, $[S_2O_8^{2-}]_0 = 0.025$ M, $[Cu^{2+}]_0 = 2.5 \times 10^{-5}$ M, $[H^+]_0 = 10^{-5}$ M, $k_0 = 1.2 \times 10^{-3}$ s^{-1}.

Figure S7. Simulation of the CSTR dynamics of the peroxodisulfate-thiosulfate-copper(II) reaction. The parameters used in the simulations are: $[S_2O_3^{2-}]_0 = 0.0025$ M, $[S_2O_8^{2-}]_0 = 0.025$ M, $[Cu^{2+}]_0 = 2.5 \times 10^{-5}$ M, $[H^+]_0 = 10^{-5}$ M, $k_0 = 1.2 \times 10^{-3}$ s^{-1}.
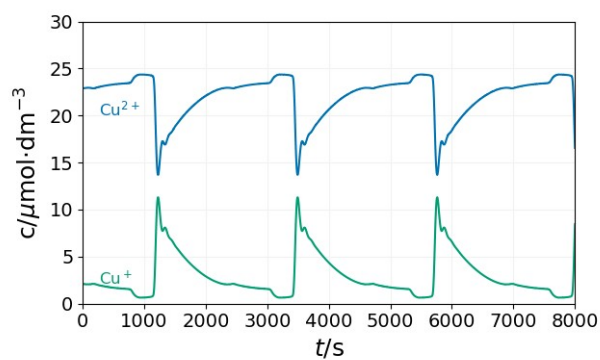

Figure S8. Simulation of the CSTR dynamics of the peroxodisulfate-thiosulfate-copper(II) reaction in presence of ammonia. The parameters used in the simulations are: $[S_2O_3^{2-}]_0 = 0.0025$ M, $[S_2O_8^{2-}]_0 = 0.025$ M, $[Cu^{2+}]_0 = 2.5 \times 10^{-5}$ M, $[H^+]_0 = 10^{-5}$ M, $[NH_3]_0 = 5 \times 10^{-4}$ M, $k_0 = 1.2 \times 10^{-3}$ s^{-1}.
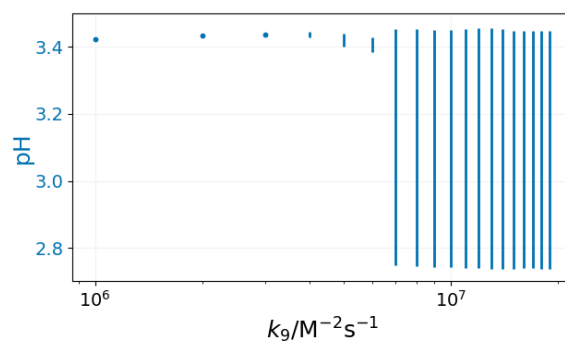
Figure S9. Simulated bifurcation diagram of the CSTR dynamics of the peroxodisulfate-thiosulfate-copper(II) reaction in absence of ammonia. The parameters used in the simulations are: $[S_2O_3^{2-}]_0 = 0.0025$ M, $[S_2O_8^{2-}]_0 = 0.025$ M, $[Cu^{2+}]_0 = 2.5 \times 10^{-5}$ M, $[H^+]_0 = 10^{-5}$ M, $k_0 = 1.2 \times 10^{-3}$ s^{-1}.
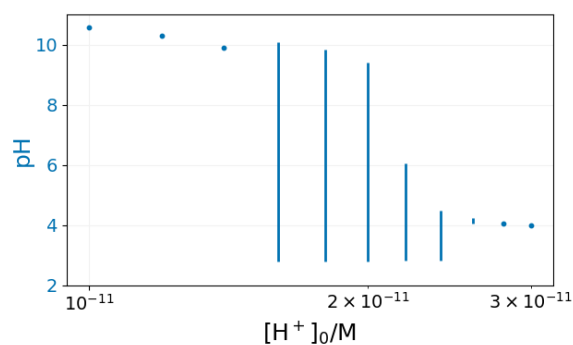

Figure S10. Simulated bifurcation diagram of the CSTR dynamics of the peroxodisulfate-thiosulfate-copper(II) reaction in absence of ammonia. The parameters used in the simulations are: $[S_2O_3^{2-}]_0 = 0.0025$ M, $[S_2O_8^{2-}]_0 = 0.025$ M, $[Cu^{2+}]_0 = 2.5 \times 10^{-5}$ M, $k_0 = 1.2 \times 10^{-3}$ s^{-1}.